JCI The Journal of Clinical Investigation

An endocannabinoid-regulated basolateral amygdala–nucleus accumbens circuit modulates sociability

Oakleigh M. Folkes, … , Brad A. Grueter, Sachin Patel

J Clin Invest. 2020;130(4):1728-1742. https://doi.org/10.1172/JCI131752.

Research Article Neuroscience

Graphical abstract

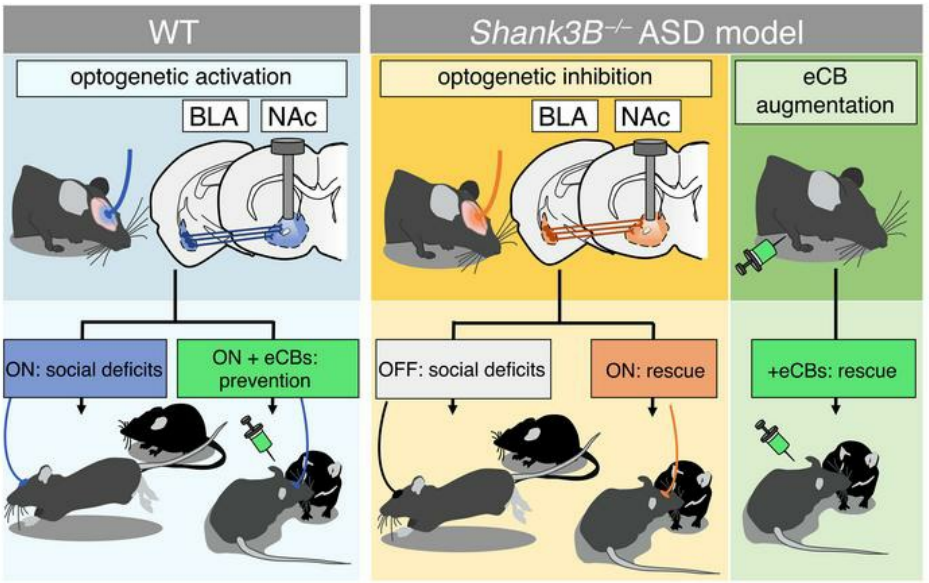

An endocannabinoid-regulated basolateral amygdala–nucleus accumbens circuit modulates sociability

Oakleigh M. Folkes,[1,2] Rita Báldi,[1] Veronika Kondev,[1,3] David J. Marcus,[1,3] Nolan D. Hartley,[1,3] Brandon D. Turner,[3,4] Jade K. Ayers,[1] Jordan J. Baechle,[1] Maya P. Misra,[1] Megan Altemus,[1] Carrie A. Grueter,[4] Brad A. Grueter,[3,4] and Sachin Patel[1,2,3,5,6]

[1]Department of Psychiatry and Behavioral Sciences, Vanderbilt University Medical Center, Nashville, Tennessee, USA. [2]Department of Pharmacology and [3]Vanderbilt Brain Institute, Vanderbilt University School of Medicine, Nashville, Tennessee, USA. [4]Department of Anesthesiology, Vanderbilt University Medical Center, Nashville, Tennessee, USA. [5]Department of Molecular Physiology and Biophysics, Vanderbilt University School of Medicine, Nashville, Tennessee, USA. [6]Vanderbilt Center for Addiction Research, Vanderbilt University School of Medicine, Nashville, Tennessee, USA.

Deficits in social interaction (SI) are a core symptom of autism spectrum disorders (ASDs); however, treatments for social deficits are notably lacking. Elucidating brain circuits and neuromodulatory signaling systems that regulate sociability could facilitate a deeper understanding of ASD pathophysiology and reveal novel treatments for ASDs. Here we found that in vivo optogenetic activation of the basolateral amygdala–nucleus accumbens (BLA-NAc) glutamatergic circuit reduced SI and increased social avoidance in mice. Furthermore, we found that 2-arachidonoylglycerol (2-AG) endocannabinoid signaling reduced BLA-NAc glutamatergic activity and that pharmacological 2-AG augmentation via administration of JZL184, a monoacylglycerol lipase inhibitor, blocked SI deficits associated with in vivo BLA-NAc stimulation. Additionally, optogenetic inhibition of the BLA-NAc circuit markedly increased SI in the *Shank3B*$^{-/-}$ mouse, an ASD model with substantial SI impairment, without affecting SI in WT mice. Finally, we demonstrated that JZL184 delivered systemically or directly to the NAc also normalized SI deficits in *Shank3B*$^{-/-}$ mice, while ex vivo JZL184 application corrected aberrant NAc excitatory and inhibitory neurotransmission and reduced BLA-NAc–elicited feed-forward inhibition of NAc neurons in *Shank3B*$^{-/-}$ mice. These data reveal circuit-level and neuromodulatory mechanisms regulating social function relevant to ASDs and suggest 2-AG augmentation could reduce social deficits via modulation of excitatory and inhibitory neurotransmission in the NAc.

Introduction

Autism spectrum disorders (ASDs) are neurodevelopmental disorders characterized by 2 core symptom domains: repetitive behaviors and abnormal social communication and social behaviors (1). Currently, there are no FDA-approved pharmacological treatments for the core symptoms of ASD. Therefore, elucidation of new therapeutic approaches is urgently needed. In particular, there is an unmet need for pharmacological treatment of social interaction and social communication deficits in ASD (2–6).

One such novel target could be the endocannabinoid (eCB) system. eCBs regulate several central nervous system functions, including motor control, repetitive behaviors, pain perception, anxiety, stress, learning and memory, and social behaviors (7, 8), all of which are implicated in ASDs (1). Regarding social behaviors, the eCB 2-arachidonoylglycerol (2-AG) has a demonstrably significant role in regulating social behavior because increasing levels of 2-AG increases social play in juvenile rats, while decreasing 2-AG decreases acquisition of social conditioned place preference (CPP) (9, 10) in mice. Despite these data, the neural circuit and synaptic mechanisms by which eCB signaling affects social function are not well understood.

In animal models, the nucleus accumbens (NAc) and amygdala are 2 central regions for eCB regulation of sociability (9, 11, 12). Canonically, the NAc enhances motivated behavior and social function via a dopamine-dependent mechanism (11, 13–16). Although disruptions in amygdala and NAc function have been demonstrated in ASDs (17–19), how amygdala-NAc circuit activity relates to sociability deficits in ASD is not well understood. Existing literature on the amygdala, specifically the basolateral amygdala (BLA), indicates that the BLA-NAc circuit regulates learned behavioral choice, including reward seeking, risk-based decision-making, fear, and depression-like behavior, all of which may contribute to changes in social approach and social behaviors (20–27). Because the BLA-NAc circuit underlies decision-making in response to rewarding cues and subsequent behavioral responses (21, 23), we hypothesize that activity in the BLA-NAc circuit may regulate multiple aspects of sociability under physiological conditions and perhaps under conditions of impaired social function.

ASD is a highly heritable neuropsychiatric disorder, as evidenced by twin and familial studies, and one of the most common genetic findings in patients with ASD are mutations in genes encoding Src homology domain 3 and multiple ankyrin repeat domains 3 (SHANK3) (28–32). SHANK3 is a postsynaptic density protein expressed in glutamatergic neurons that serves as a scaffold for key glutamatergic receptors (33, 34). The *Shank3B*$^{-/-}$ mouse model is characterized by an excision of exons 13–16 that causes removal of 2 major *Shank3* isoforms and replicates the genetic findings commonly presented in patients (33, 35–38).

Conflict of interest: SP has received research contract support from H. Lundbeck A/S in the past 3 years. SP has received consultation fees from Psy Therapeutics.

Submitted: July 14, 2019; **Accepted:** December 18, 2019; **Published:** February 24, 2020.
Reference information: *J Clin Invest*. 2020;130(4):1728–1742.
https://doi.org/10.1172/JCI131752.

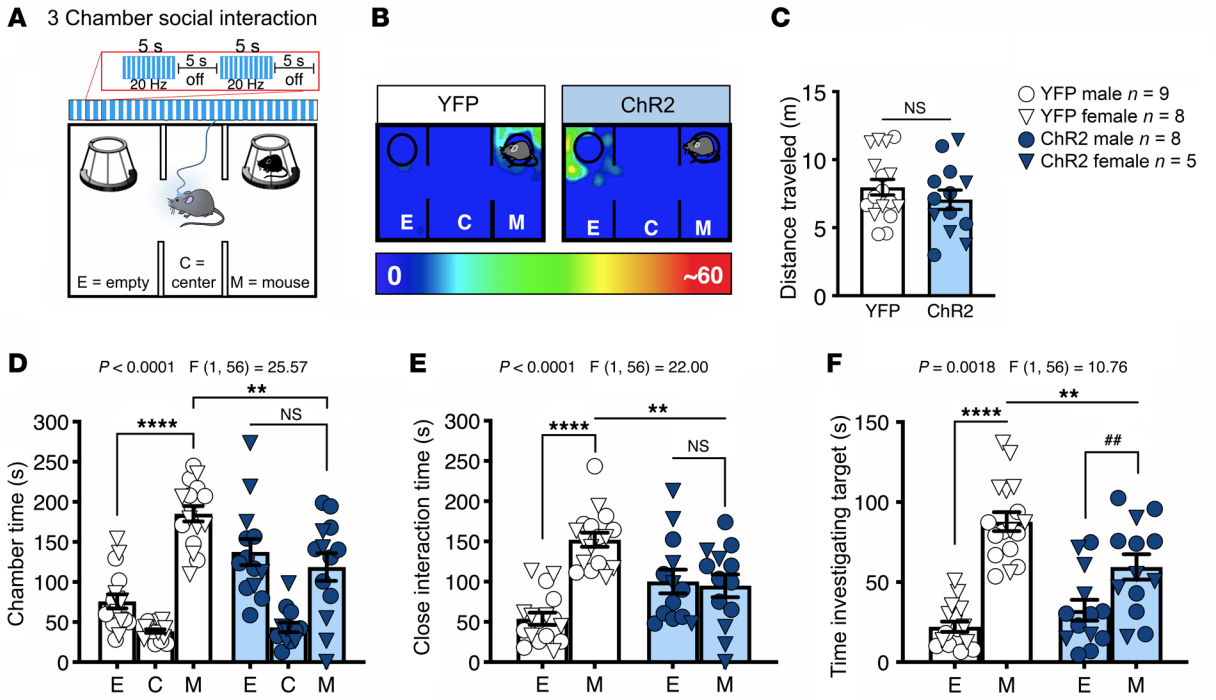

Figure 1. Activation of BLA terminals in the NAc decreases sociability. (**A**) Three-chamber SI task and optogenetic stimulation protocol. Animals were continuously stimulated during the 5-minute test using a 20-Hz pattern (10 mW, 5 seconds on and 5 seconds off). (**B**) Representative heatmaps of chamber time in a ChR2-expressing and YFP-expressing control mouse. (**C**) Optogenetic stimulation of the BLA-NAc circuit did not affect distance traveled (NS, $P = 0.3224$). (**D**) Animals that express ChR2 showed reduced social preference (**$P = 0.0010$, ****$P < 0.0001$, and NS, $P = 0.5565$), (**E**) decreased close interaction time (**$P = 0.0011$, ****$P < 0.0001$, and NS, $P = 0.9353$), and (**F**) reduced time investigating, or sniffing, the target mouse compared with animals that express YFP (M-M **$P = 0.0026$, E-M ****$P < 0.001$, and ##$P = 0.0071$). YFP $n = 17$, and ChR2 $n = 13$ (**C**–**F**). Data analyzed via 2-way mixed-effects ANOVA followed by Holm-Šídák multiple-comparisons test (**D**–**F**) or unpaired, 2-tailed t test (**C**). P and F values for chamber × virus interaction shown in **D**–**F**.

This excision results in a loss of function of the SHANK3 protein. *Shank3B*$^{-/-}$ mice demonstrate excessive, repetitive grooming and deficits in social behavior, making the model a good candidate for exploring novel ASD therapeutic targets and circuit dysfunction (39, 40). Previous studies suggest that the significant changes in social behavior in the *Shank3* loss-of-function models may be mediated by signaling changes in the NAc (41), warranting further investigation of the NAc and NAc-associated circuitry in the regulation of social function and pathophysiology of ASD.

Here we used optogenetic circuit mapping to demonstrate that activation of the BLA-NAc circuit disrupted physiological social function and that inhibition of this circuit reversed social deficits in *Shank3B*$^{-/-}$ mice. We further demonstrated that 2-AG signaling is a negative regulator of BLA-NAc glutamatergic transmission and that pharmacological augmentation of 2-AG levels mitigated social avoidance induced by BLA-NAc circuit activation and social avoidance behavior observed in *Shank3B*$^{-/-}$ mice, possibly via decreasing BLA-NAc–elicited feed-forward inhibition.

Results

Optogenetic activation of the BLA-NAc circuit disrupts social behavior. To examine the role of the BLA-NAc circuit in social function, we used an in vivo optogenetic approach in which we injected a ChR2 [AAV5-CaMKIIa-hChR2(H134)-EYFP] viral vector into the BLA and delivered blue light stimulation into the NAc via fiber optic cannulas. First, we tested the effects of 20-Hz blue light stimulation (5-ms light pulses, 10–13 mW, 5 seconds on and 5 seconds off) on social function using the 3-chamber social interaction (SI) task in male and female C57BL/6J mice. We found that blue light delivery into the NAc impaired sociability in ChR2-expressing compared with yellow fluorescent protein–expressing (YFP-expressing) (AAV5-CaMKIIa-EYFP) control animals (Figure 1, A and B; and Supplemental Figure 1, A and B for cannula placements; supplemental material available online with this article; https://doi.org/10.1172/JCI131752DS1). This light stimulation pattern did not affect distance traveled in this apparatus (Figure 1C) but significantly decreased time ChR2-expressing mice spent in the social chamber relative to YFP-expressing mice (Figure 1D). We also found that ChR2-expressing mice, relative to YFP controls, spent significantly less time in proximity (5 cm) to the target animals (Figure 1E) and spent less time sniffing or investigating the cup in which the target mouse was contained (Figure 1F). Importantly, BLA-NAc stimulation for 5 minutes before the 3-chamber SI task did not alter sociability (Supplemental Figure 2, A and B), suggesting that the sociability-impairing effects of BLA-NAc activation required ongoing circuit stimulation. We next validated our optogenetic stimulation protocol using ex vivo whole-cell electrophysiological recordings. These studies revealed 20-Hz blue light stimulation within the NAc triggered high-fidelity neuronal firing, confirming that this frequency of stimulation increased NAc neuronal activity and increased spontaneous glutamate release onto NAc medium spiny neurons (MSNs) (Supplemental Figure 3, A–E).

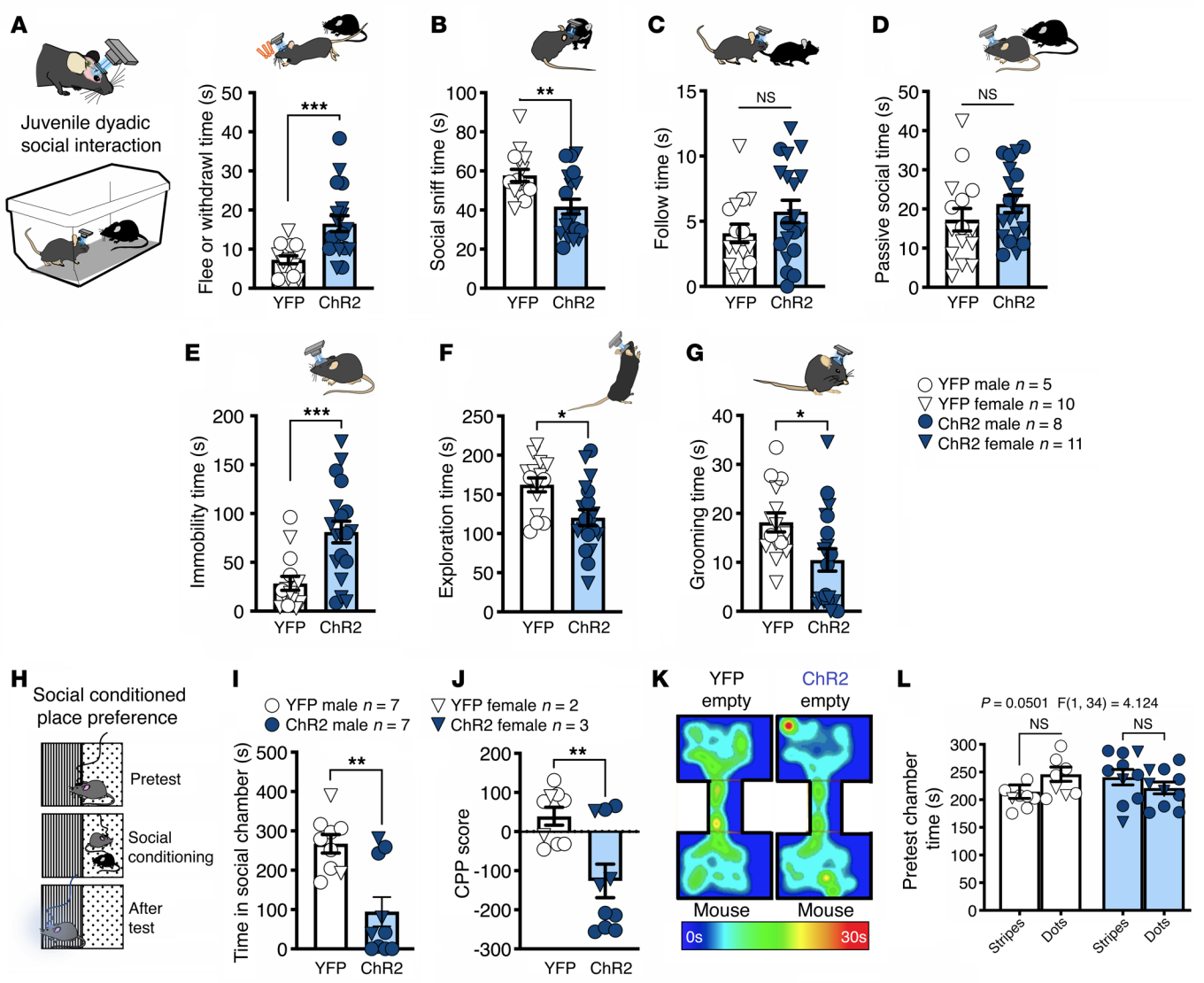

Figure 2. Activation of BLA terminals in the NAc increases social avoidance and reduces SI seeking. (**A**) Optogenetic stimulation of the BLA-NAc circuit increased fleeing and withdrawal behaviors (***P = 0.0007) and (**B**) decreased social sniffing behaviors (**P = 0.0041) compared with YFP-expressing controls. There was no effect of BLA-NAc activation on (**C**) following (P = 0.1573) or (**D**) passive social behavior (P = 0.2604). Animals expressing ChR2 were significantly more (**E**) immobile (***P = 0.0007) and (**F**) explored less (*P = 0.0049) than YFP controls. (**G**) Animals that expressed ChR2 self-groomed significantly less than YFP-expressing controls (*P = 0.0184). YFP n = 15, and ChR2 n = 19 (**A**–**G**). (**H**) Social CPP paradigm. (**I**) Bilateral activation of the BLA-NAc circuit significantly decreased time in the social-paired chamber during the posttest (**P = 0.0013) (**J**) and reduced CPP score relative to YFP controls (**P = 0.0041). (**K**) Representative heatmaps for the social CPP experiment. (**L**) No pretest preference to either chamber was detected (YFP dots vs. stripes, P = 0.1777; ChR2 dots vs. stripes, P = 0.4619). YFP n = 9, and ChR2 n = 10 (**I**, **J**, **L**). Data analyzed via unpaired, 2-tailed t test (**A**–**G**, **I**, and **J**) or 2-way mixed-effects ANOVA with Holm-Šídák multiple-comparisons post hoc test (**L**), with P and F values for chamber × virus interaction shown in **L**.

Optogenetic stimulation of BLA afferents to the NAc also resulted in optically evoked excitatory postsynaptic currents (oEPSCs) onto D2 dopamine receptor–expressing MSNs ($D2^+$ MSNs), and $D2^-$ (presumptive D1) MSNs, indicating BLA glutamatergic afferents to the NAc target both subtypes equally (Supplemental Figure 3, F–H). Last, we sought to determine whether BLA-NAc activity could bidirectionally modulate sociability. Thus, we repeated the 3-chamber SI task in animals that bilaterally expressed either NpHR (AAV5-CaMKIIa-eNpHR3.0-EYFP) or YFP to inhibit BLA-NAc activity in vivo (Supplemental Figure 2E). However, we found no effects of constant orange light (620 nm, 10–13 mW) inhibition of the BLA-NAc circuit on sociability in the 3-chamber SI test (Supplemental Figure 2, F and G), suggesting BLA-NAc activity is not necessary for physiological expression of SI.

To extend the observation that BLA-NAc activation disrupts sociability, we next analyzed the effects of BLA-NAc activation in a juvenile reciprocal SI test using a wireless in vivo optogenetic system (Figure 2). In this task, we found that unilateral, 20-Hz blue light stimulation significantly increased time fleeing or withdrawing from the social target (Figure 2A) and decreased time spent socially sniffing (Figure 2B) in mice that expressed ChR2 relative to YFP controls. In contrast, we found no effects of blue light stimulation in ChR2-expressing compared to YFP-expressing controls on the time the test animals spent following the social tar-

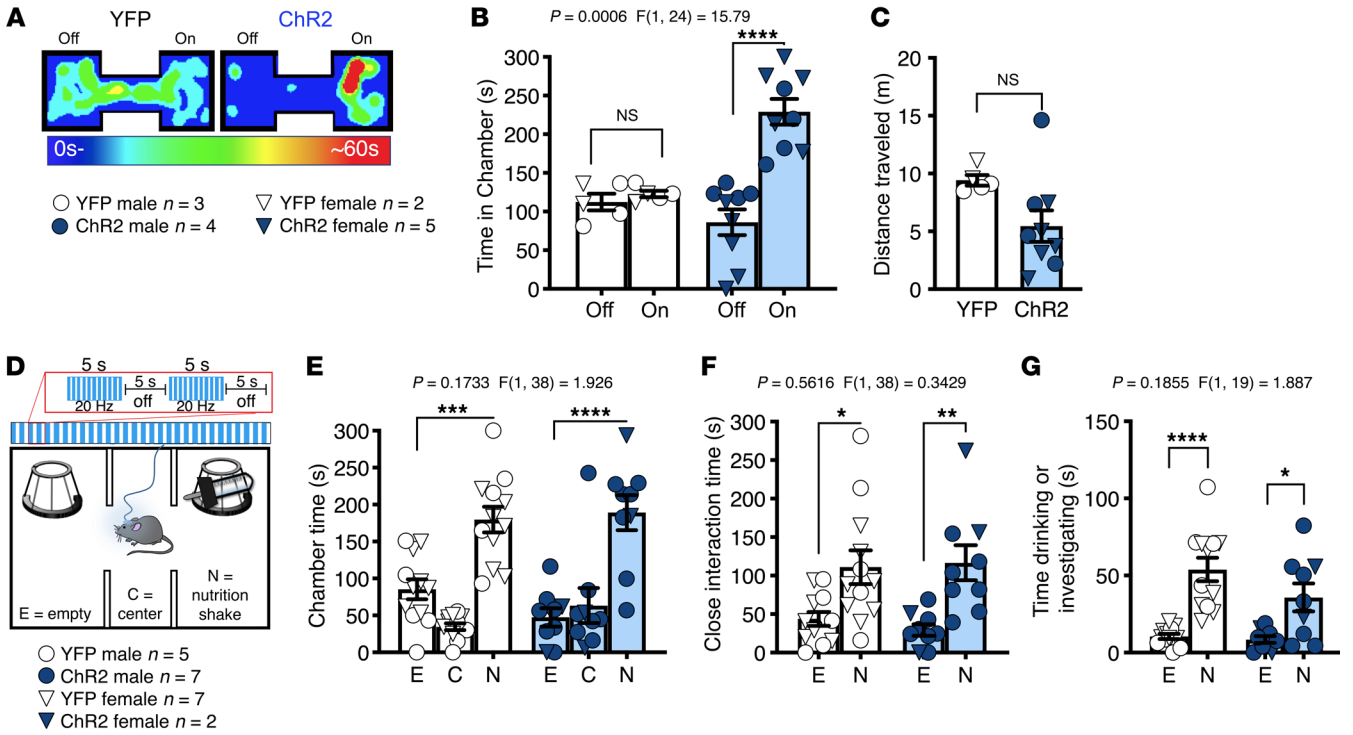

Figure 3. Activation of BLA terminals in the NAc is rewarding but does not reduce palatable food seeking. (**A**–**C**) Effects of BLA-NAc stimulation in the RtPP assay. (**A**) Representative heatmaps of RtPP results. (**B** and **C**) Animals expressing ChR2 spent significantly more time in the stimulation-paired (On) compared with nonpaired (Off) side in the RtPP assay (NS, $P = 0.9083$, and $^{****}P < 0.0001$) without any effect on total distance traveled (unpaired, 2-tailed t test, $P = 0.0568$). YFP $n = 5$, and ChR2 $n = 9$ (**B** and **C**). (**D**–**G**) Effects of BLA-NAc stimulation on Ensure-seeking behavior. (**D**) In a modified 3-chamber task a sipper bottle of Ensure was added to 1 chamber while stimulation was delivered to animals. (**E**) Activation of the BLA-NAc circuit did not alter time spent in the chamber with ($^{***}P = 0.0003$, and $^{****}P < 0.0001$), (**F**) close to ($^{*}P = 0.0102$, and $^{**}P = 0.0037$), or (**G**) drinking ($^{****}P < 0.0001$, and $^{*}P = 0.0128$) the nutrition shake in ChR2-expressing animals compared to YFP-expressing animals. YFP $n = 12$, and ChR2 $n = 9$ (**E**–**G**). Data analyzed via unpaired, 2-tailed t test (**C**) or 2-way mixed-effects ANOVA with Holm-Šídák multiple-comparison post hoc tests (**B**, **E**–**G**), with P and F values for chamber × virus interaction shown in **B**, and **E**–**G**.

get (Figure 2C) or engaged in passive social behavior (Figure 2D). Last, immobility time was increased (Figure 2E) while exploration time (Figure 2F) and self-grooming (Figure 2G) were decreased in ChR2 animals compared with YFP-expressing controls. These data are consistent with our 3-chamber SI data and indicate that BLA-NAc pathway activation reduces social behavior and induces social avoidance in a more naturalistic setting.

We next tested the effects of BLA-NAc activation on motivational aspects of SI seeking using a social CPP task (Figure 2H). After conditioning, we found that bilateral (but not unilateral, Supplemental Figure 2, C and D) blue light delivery during social CPP testing resulted in decreased time spent in the social-paired chamber and lower CPP scores (posttest chamber time minus pretest chamber time) (Figure 2, I–K) in ChR2-expressing animals compared with YFP-expressing controls. Of note, virus expression did not alter pretest chamber preference (Figure 2L). Taken together, data from these 3 assays indicate BLA-N.0Ac activation impairs motivational aspects of SI seeking, reduces social preference, and induces social avoidance, in male and female mice.

Optogenetic activation of the BLA-NAc circuit is rewarding but not anxiogenic. The NAc is well known to regulate reward-related processes (42, 43), suggesting BLA-NAc stimulation could reduce sociability via an occlusion of the rewarding aspects of SI. To examine this possibility, we first tested the reinforcing effects of BLA-NAc stimulation using a real-time place preference (RtPP) assay. Consistent with previous studies (24), we found animals expressing ChR2 spent more time in the ON chamber, in which blue light stimulation was delivered, versus the OFF chamber in the RtPP task (Figure 3, A and B), without significantly affecting locomotor activity (Figure 3C). Taken with our previous data above, these results indicated BLA-NAc glutamatergic circuits can support RtPP and social avoidance in parallel. These data also suggest BLA-NAc stimulation could indeed impair social function via occlusion of the rewarding aspects of social behavior. If this were the case, one would also predict occlusion of natural reward-seeking behavior, such as food seeking, by BLA-NAc stimulation. To test this hypothesis more explicitly, we measured time in a chamber containing a highly palatable food (vanilla Ensure) in lieu of a social target in a modified 3-chamber task design (Figure 3D). In this task we observed BLA-NAc stimulation did not disrupt chamber preference (Figure 3E), alter time spent in proximity to the Ensure-containing cup (Figure 3F), or affect time spent drinking Ensure (Figure 3G). Overall these data suggest BLA-NAc activation does not reduce sociability via occlusion of the rewarding aspects of SI. Additionally, because changes in anxiety and anxiety-like behavior can affect social behavior (1, 44, 45), we next tested the effects of BLA-NAc stimulation on anxiety-like behavior and found activation did not alter behavior in the light-dark

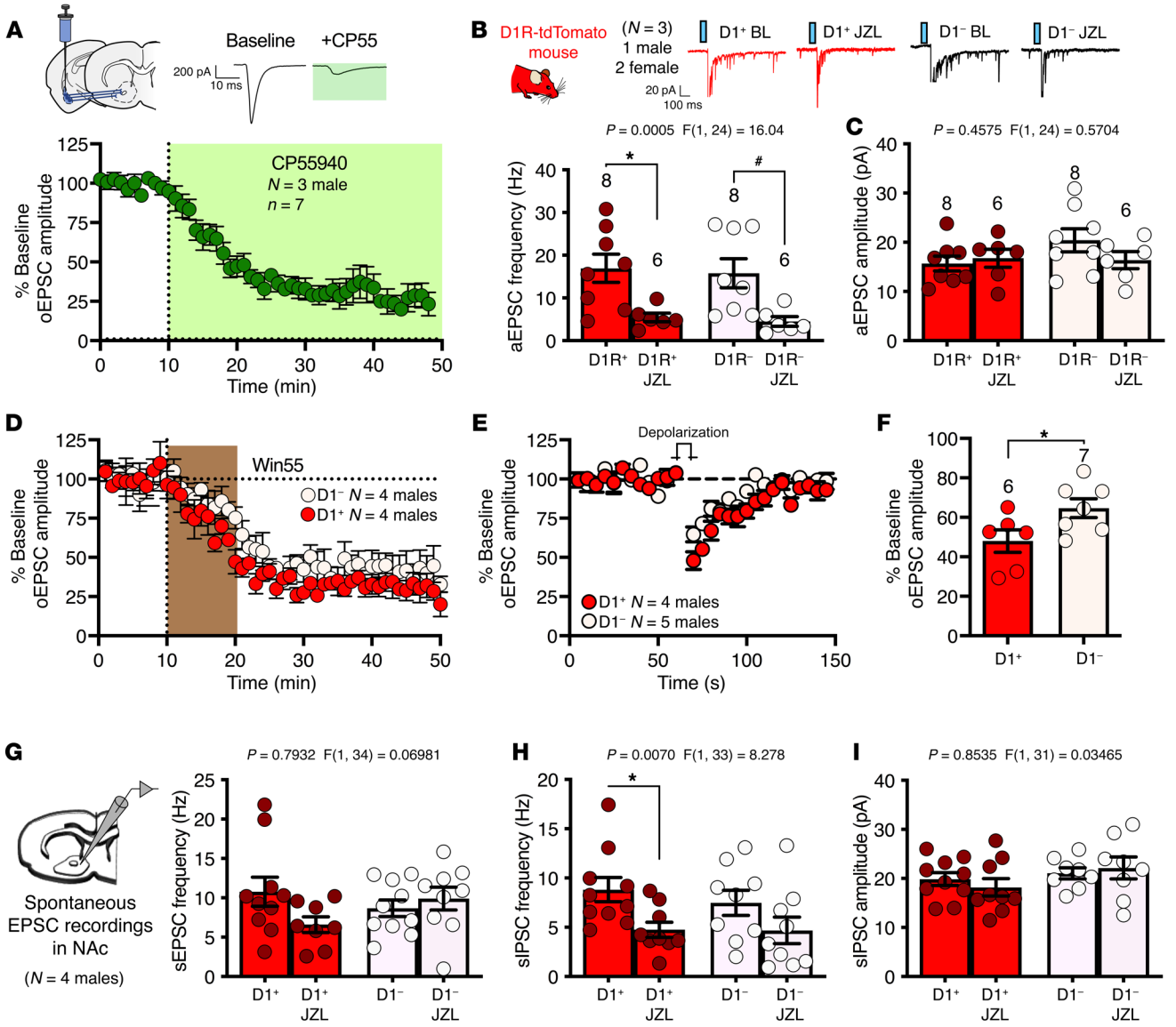

Figure 4. CB1 receptors and 2-AG augmentation regulate BLA-NAc synapses. (**A**) The cannabinoid receptor agonist CP55940 decreased oEPSC amplitude in the NAc; $N = 3$. (**B**) JZL184 reduced aEPSC frequency in D1 receptor$^+$ (D1R$^+$; $^*P = 0.0171$) and D1 receptor$^-$ (D1R$^-$) cells ($^\#P = 0.0197$) (**C**) but did not affect aEPSC amplitude after BLA-NAc optogenetic stimulation; D1$^+$ $n = 3$, and D1$^-$ $n = 3$ (**B**, **C**). aEPSC, asynchronous excitatory postsynaptic current; BL, baseline. (**D**) WIN55212-2 (Win55), a cannabinoid receptor agonist, uniformly decreased oEPSC amplitude in D1$^+$ and D1$^-$ NAc cell types; D1$^+$ $n = 4$, and D1$^-$ $n = 4$. (**E**) DSE was present in both D1$^+$ and D1$^-$ NAc cells, (**F**) although DSE magnitude was increased in D1$^+$ compared with D1$^-$ cells ($^*P = 0.0450$); D1$^+$ $n = 4$, and D1$^-$ $n = 5$ (**E**, **F**). (**G**) sEPSC frequency in NAc recordings were unaffected by JZL184, (**H**) but there was a significant effect of JZL184 on sIPSC frequency ($^*P = 0.0400$). (**I**) There were no effects of JZL184 on sIPSC amplitude; D1$^+$ $n = 4$, D1$^-$ $n = 4$. Data analyzed via 2-way mixed-effects ANOVA followed by Holm-Šídák multiple-comparisons test (**B**, **C**, **G**–**I**) or unpaired, 2-tailed t test (**F**). P and F values for drug effect shown in **B**, **C**, and **G**–**I**.

box (Supplemental Figure 4, A–D), and neither activation nor inhibition affected anxiety-like behavior in the elevated plus maze (Supplemental Figure 4, E–L). Taken together, these data indicate social avoidance observed during BLA-NAc stimulation was not secondary to increased anxiety-like behavior.

eCB signaling broadly regulates BLA-NAc glutamatergic transmission. Given the prominent role of eCB signaling in the regulation of central glutamatergic transmission (46), and the role of eCB signaling in social function (11, 12, 47), we next examined the possibility that eCB signaling regulates BLA-NAc glutamatergic activity. Indeed, the cannabinoid receptor agonist CP55940 significantly decreased oEPSC amplitude at BLA-NAc synapses, supporting the presence of functional cannabinoid receptors in this pathway (Figure 4A). Because previous investigations have shown differential eCB signaling at glutamatergic synapses onto distinct striatal MSN subtypes and within distinct BLA-NAc subcircuits (24, 48–50), we further examined the effect of 2-AG signaling and cannabinoid receptor 1 (CB1) function at BLA-NAc D1$^+$ and D1$^-$ (presumptive D2) MSN glutamatergic synapses. We first found that increasing 2-AG levels via inhibition of monoacylglycerol lipase (MAGL) with the inhibitor JZL184 significantly reduced the frequency, but not amplitude, of asynchronous EPSCs onto both

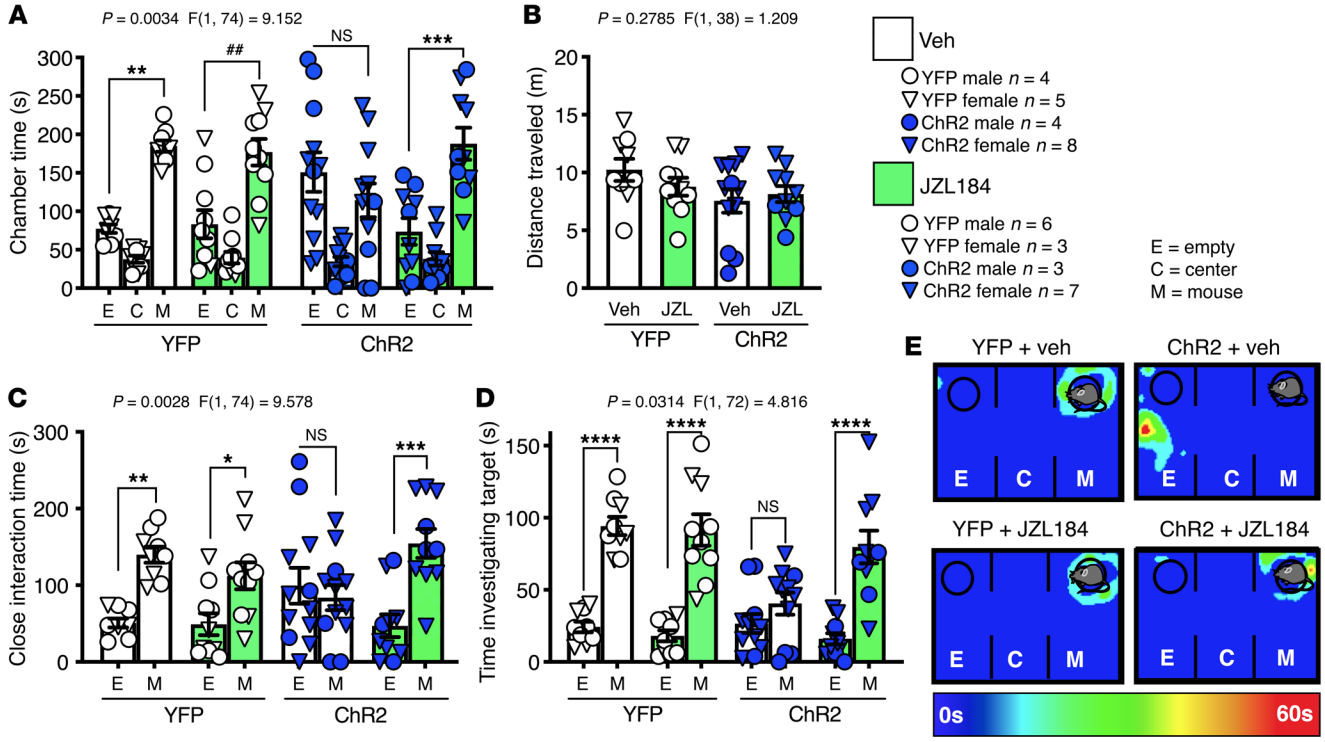

Figure 5. JZL184 pretreatment blocks BLA-NAc activation–induced decreases in sociability. (**A**) YFP-expressing animals that received JZL184 (JZL) or vehicle (Veh) treatment showed a social preference (Veh: $^{**}P = 0.0015$; JZL: $^{\#\#}P = 0.0041$), (**C**) spent more time in the close interaction zone (Veh: $^{**}P = 0.0032$; JZL: $^{*}P = 0.0429$), and (**D**) and spent increased time investigating the mouse, relative to empty, target (Veh: $^{****}P < 0.0001$; JZL: $^{****}P < 0.0001$). ChR2 animals pretreated with Veh had no (**A**) social chamber preference (NS, $P = 0.4699$), (**C**) preference for time spent near the target (NS, $P = 0.9302$), or (**D**) increased time investigating the mouse, relative to empty, target (NS, $P = 0.5315$). ChR2 animals treated with JZL184 had a significant preference for the (**A**) mouse chamber ($^{***}P = 0.0003$) (**C**) and spent increased time in close interaction ($^{***}P = 0.0001$) and (**D**) investigating the mouse, relative to empty, target ($^{****}P < 0.0001$). (**B**) There was no effect of virus or drug treatment on distance traveled. (**E**) Representative heatmaps of each treatment condition. YFP + Veh $n = 9$, YFP + JZL184 $n = 9$, ChR2 + Veh $n = 12$, and ChR2 + JZL184 $n = 10$ (**A**–**D**). Data analyzed via 3-way mixed-effects ANOVA followed by Holm-Šídák multiple-comparisons test (**A**, **C**, **D**) or 2-way ANOVA with Holm-Šídák multiple-comparisons test (**B**). *P* and *F* values for chamber × virus × drug interaction shown in **A**, **C**, and **D** or virus × drug (**B**).

$D1^+$ and $D1^-$ NAc MSNs (Figure 4, B and C) and that WIN55212-2, another direct cannabinoid receptor agonist, resulted in suppression of oEPSC amplitude and long-term depression onto both $D1^+$ and $D1^-$ MSNs (Figure 4D). We next investigated the expression of depolarization-induced suppression of excitation (DSE), a protocol used to measure endogenous retrograde synaptic 2-AG signaling, and found DSE was present at both BLA to $D1^+$ and $D1^-$ MSN synapses (Figure 4E), although the suppression was more robust in $D1^+$ relative to $D1^-$ MSNs (Figure 4F). Last, we examined the role of JZL184 on spontaneous synaptic activity in the NAc. JZL184 did not alter spontaneous EPSC (sEPSC) frequency onto either $D1^+$ or $D1^-$ MSNs (Figure 4G) but significantly decreased spontaneous inhibitory postsynaptic current (sIPSC) frequency, via post hoc analysis for $D1^+$ MSNs (Figure 4H). There was no effect of JZL184 on $D1^+$ or $D1^-$ sIPSC amplitude (Figure 4I). These data suggest that eCB regulation of BLA-NAc glutamatergic transmission is present on both primary MSN cell types in the NAc and that 2-AG signaling can affect NAc local GABAergic neurotransmission.

2-AG augmentation prevents BLA-NAc activation-induced social impairment. Our data thus far suggest 2-AG signaling can reduce presynaptic glutamate release at BLA-NAc synapses, suggesting that pharmacological 2-AG augmentation could counteract the social impairment observed after BLA-NAc circuit activation. To test this hypothesis, we administered JZL184 (8 mg/kg i.p.) 1 hour before BLA-NAc stimulation in the 3-chamber SI task. We found that JZL184 prevented blue light delivery–dependent suppression of sociability in the 3-chamber SI test in ChR2-expressing animals but did not affect SI in YFP-expressing controls (Figure 5A); JZL184 did not affect distance traveled in this assay (Figure 5B). ChR2-expressing JZL184-treated mice also spent more time in the close interaction zone of the 3-chamber apparatus (Figure 5C) and more time investigating the mouse-containing cup relative to the empty cup (Figure 5, D and E) compared with vehicle-treated ChR2-expressing mice. Last, neither pharmacologically increasing (JZL184 8 mg/kg i.p.) nor pharmacologically decreasing (DO34 50 mg/kg i.p.) 2-AG levels affected SI in naive, nonsurgical animals (Supplemental Figure 5, A–D). These data indicate that, while pharmacological modulation of 2-AG levels has little effect on physiological expression of sociability, 2-AG augmentation is able to attenuate the social avoidance behavior induced by BLA-NAc circuit activation.

Optogenetic BLA-NAc circuit inhibition reduces social deficits in Shank3B$^{-/-}$ mice. That BLA-NAc inhibition did not affect social behavior in WT mice (see Supplemental Figure 2) suggests that the BLA-NAc circuit does not physiologically regulate sociability under basal conditions. However, it is possible that BLA-NAc

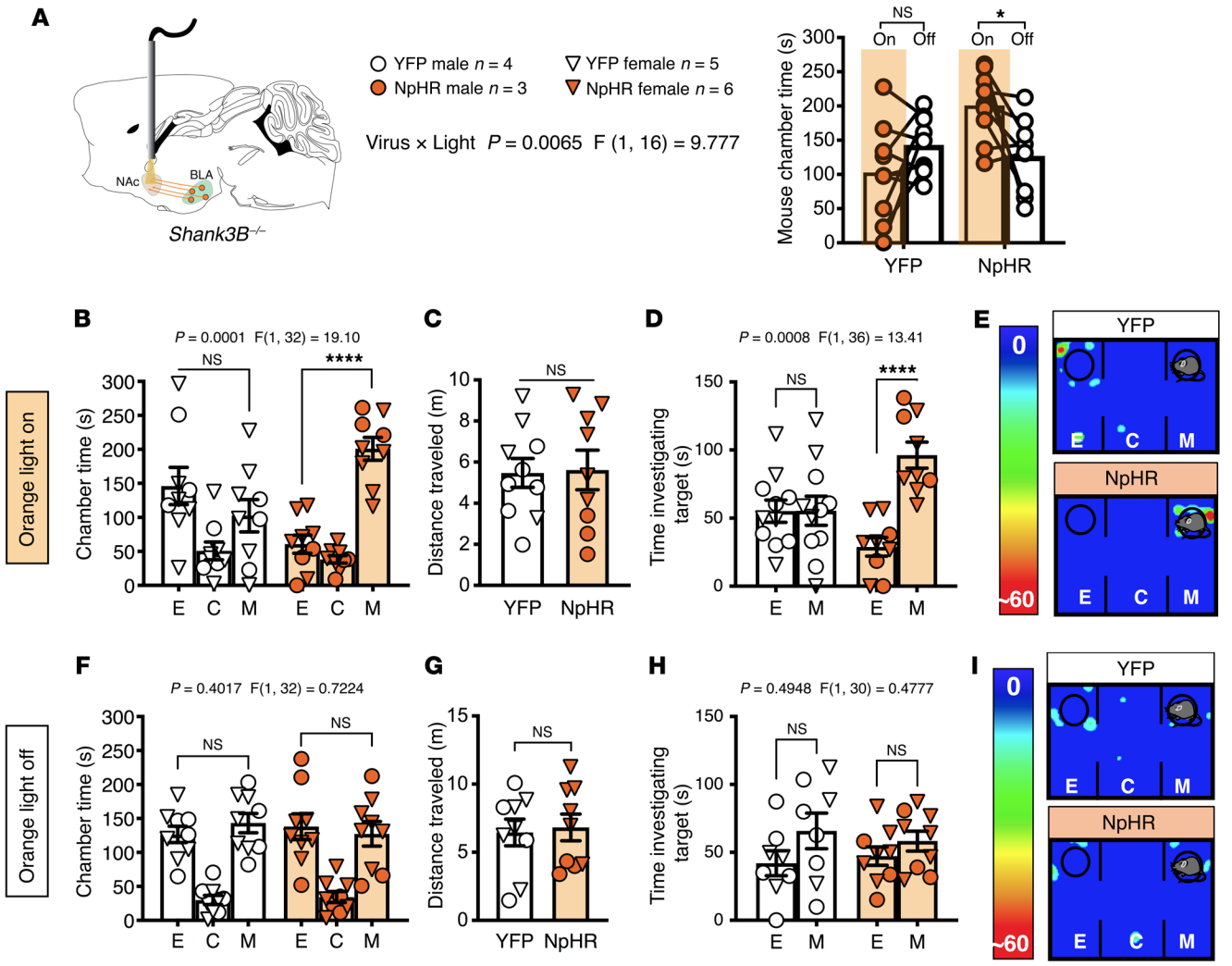

Figure 6. Inhibition of the BLA-NAc circuit normalized SI deficits in *Shank3B*$^{-/-}$ mice. (**A**) *Shank3B*$^{-/-}$ mice expressing NpHR in the BLA with bilateral orange light stimulation delivered to the NAc spent significantly more time in the mouse chamber during orange light delivery (On) compared with light Off conditions (*P = 0.0230). YFP animals did not show a preference for the mouse chamber (NS, P = 0.2529). (**B**) *Shank3B*$^{-/-}$ mice expressing YFP under light On conditions did not exhibit social preference (NS, P = 0.2831), while animals that express NpHR had a preference for the mouse chamber (****P < 0.0001). (**C**) No effect on distance traveled was observed (NS, P = 0.9057) in the light On paradigm. (**D**) Mice that express NpHR had a significant increase in time investigating the mouse cup under light On conditions (****P < 0.0001). (**E**) Representative heatmaps under light On conditions. (**F**) Neither YFP (NS, P = 0.7166) nor NpHR (NS, P = 0.8731) *Shank3B*$^{-/-}$ mice showed mouse chamber preference (**H**) or preference for time investigating the mouse target (YFP NS, P = 0.1617; NpHR NS, P = 0.6193) under light Off conditions. (**G**) There were no effects on distance traveled under light Off conditions (P = 0.7959). (**I**) Representative heatmaps under light Off conditions. YFP n = 9, and NpHR n = 9 (**B**–**D**, **F**–**H**). Data analyzed via 2-way mixed-effects ANOVA with Holm-Šídák multiple-comparisons test (**A**, **B**, **D**, **F**, **H**) or unpaired, 2-tailed t test (**C**, **G**). P and F values for light × virus interaction shown in **A** and chamber × virus interaction shown in **B**, **D**, **F**, and **H**.

activity could contribute to social impairment under pathological conditions, such as those observed in the *Shank3B*$^{-/-}$ model of syndromic ASD. Indeed, we found, using a counterbalanced crossover design, that bilateral orange light stimulation of NpHR, and thus inhibition of the BLA-NAc circuit, normalized time in the mouse chamber during orange light ON relative to light OFF testing in *Shank3B*$^{-/-}$ mice (Figure 6A; see Supplemental Figure 1, C and D, for cannula placements). Consistent with previous data, YFP-expressing *Shank3B*$^{-/-}$ controls showed a lack of sociability (39, 51, 52) under both light ON and light OFF conditions in the 3-chamber test, while NpHR-expressing *Shank3B*$^{-/-}$ mice exhibited social chamber preference only under light ON conditions (Figure 6, B, E, F, and I). There were no changes in the distance traveled between groups (Figure 6, C and G). Orange light inhibition of the BLA-NAc circuit in *Shank3B*$^{-/-}$ mice also resulted in a significant preference for time investigating the mouse-containing cup in NpHR-expressing mice under light ON, but not light OFF, condition, while YFP-expressing mice showed no preference under either condition (Figure 6, D and H). These data support the hypothesis that reducing BLA-NAc activity can enhance sociability under pathological conditions associated with reduced SI, such as those observed in the *Shank3B*$^{-/-}$ model.

2-AG augmentation reduces social deficits and feed-forward GABAergic signaling in Shank3B$^{-/-}$ *mice*. Finally, because acute treatment with JZL184 was able to reverse the sociability deficits resulting from overactivation of the BLA-NAc circuit, and inhib-

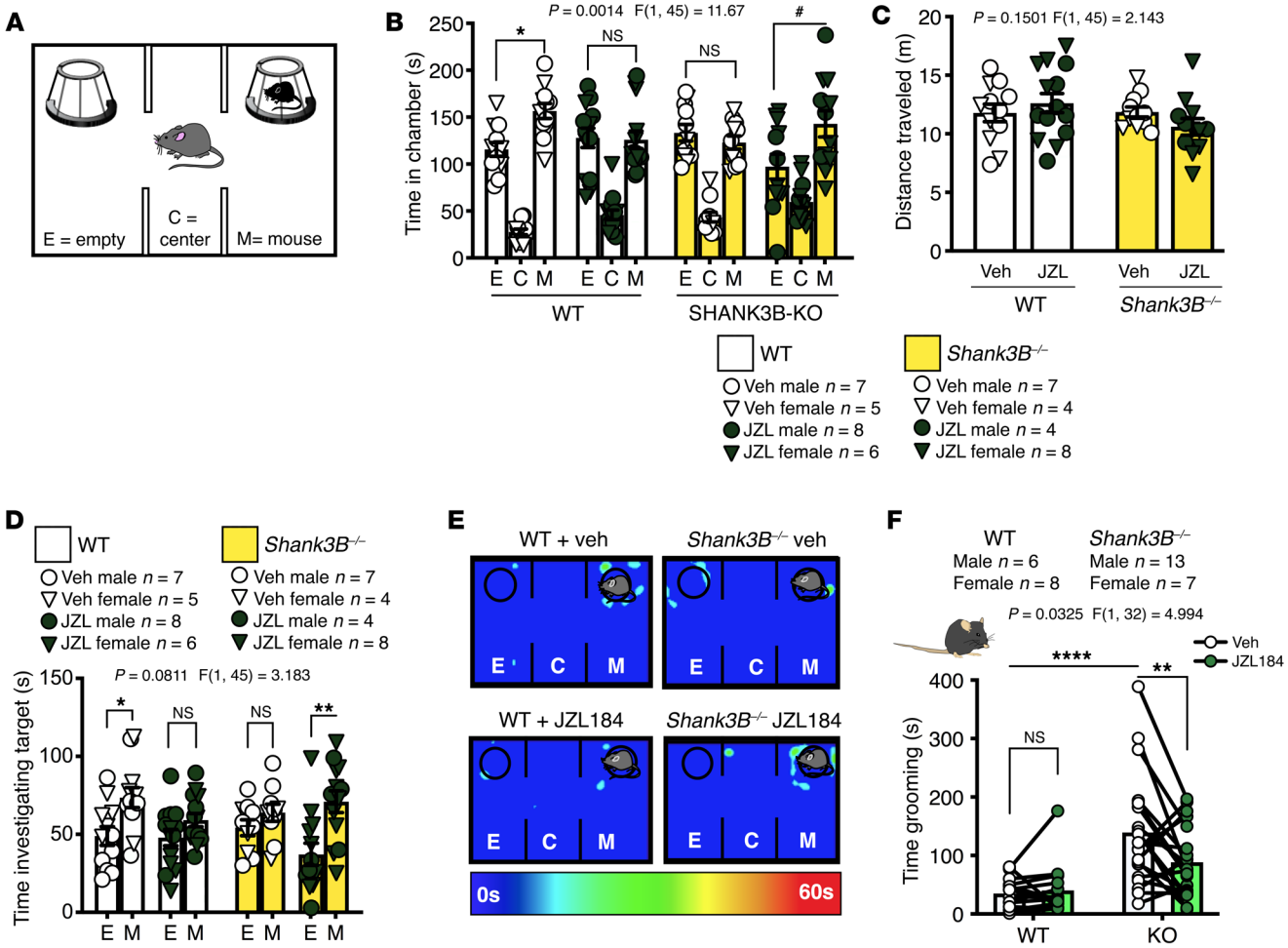

Figure 7. Systemic JZL184 treatment reverses the core behavioral abnormalities in *Shank3B*$^{-/-}$ animals. (**A**) Diagram of 3-chamber SI task. (**B**) Veh treatment did not affect SI in WT mice (*P = 0.0291 and did not induce a preference in *Shank3B*$^{-/-}$ (NS, P = 0.9369), while JZL184 eliminated social preference in WT mice (NS, P = 0.9998) but resulted in significant social preference in *Shank3B*$^{-/-}$ animals ($^{\#}P$ = 0.0122). (**C**) There was no difference in distance traveled between groups. (**D**) JZL184-treated *Shank3B*$^{-/-}$ animals (**P = 0.0016) and Veh-treated WT mice (*P = 0.0225) had a preference for investigating the mouse, over empty, target while JZL184 WT (NS, P = 0.2997) and Veh *Shank3B*$^{-/-}$ mice (NS, P = 0.4555) did not; WT + Veh n = 12, WT + JZL n = 14, KO + Veh n = 11, and KO + JZL n = 12 (**B**–**D**). (**E**) Representative heatmaps of the 3-chamber SI task. (**F**) *Shank3B*$^{-/-}$ mice treated with Veh spent significantly more time grooming compared with WT Veh animals (****P < 0.0001). *Shank3B*$^{-/-}$ mice treated with JZL184 spent significantly less time grooming compared with Veh treatment (**P = 0.0069) and WT Veh treatment, while JZL184 had no effect in WT mice (NS, P = 0.9548); WT n = 14 (6 male and 8 female), and KO n = 20 (13 male and 7 female). Data analyzed via 3-way mixed-effects ANOVA with Holm-Šídák multiple-comparisons test (**B**, **D**), 2-way ANOVA with Holm-Šídák multiple-comparisons test (**C**), or 2-way repeated-measures ANOVA with Holm-Šídák multiple-comparisons test (**F**). P and F values for chamber × genotype × drug interaction shown in **B** and **D** or genotype × drug interaction (**C**, **F**).

iting the BLA-NAc circuit reversed social deficits in *Shank3B*$^{-/-}$ mice, we hypothesized that acute treatment with JZL184 (8 mg/kg i.p.) would increase social behavior in *Shank3B*$^{-/-}$ mice (Figure 7A). Although vehicle treatment did not increase SI in *Shank3B*$^{-/-}$ animals, JZL184 pretreatment resulted in significant social preference in *Shank3B*$^{-/-}$ animals in the 3-chamber SI task (Figure 7, B–E) but had no effect on distance traveled (Figure 7C). JZL184 treatment also resulted in a preference for investigating the target mouse relative to the empty cup in *Shank3B*$^{-/-}$ mice (Figure 7D). In addition to social deficits, *Shank3B*$^{-/-}$ animals display aberrant repetitive grooming behavior (39, 51, 52), modeling the second core feature of ASDs: restricted and repetitive behaviors. We subsequently demonstrated that the amount of time grooming was significantly reduced by JZL184 (8 mg/kg i.p.) treatment in *Shank3B*$^{-/-}$ animals but did not affect grooming behavior in WT mice (Figure 7F).

Although our data clearly show systemic pharmacological augmentation of 2-AG reduced social impairment upon BLA-NAc stimulation, and in *Shank3B*$^{-/-}$ mice, these data do not conclusively link the 2 findings in a manner that supports the site of action of JZL184 as being within the BLA-NAc circuit. To directly test the hypothesis that systemic JZL184 administration effectively reduces social impairment via NAc-mediated mechanisms, we administered JZL184 (5 μg/μL) or vehicle directly into the NAc using a microinfusion approach before conducting the 3-chamber SI task in *Shank3B*$^{-/-}$ mice (Figure 8A; see Supplemental Figure 1E for cannula placements). JZL184 microinfusion did not affect distance traveled in this task (Figure 8B); however, it increased time *Shank3B*$^{-/-}$

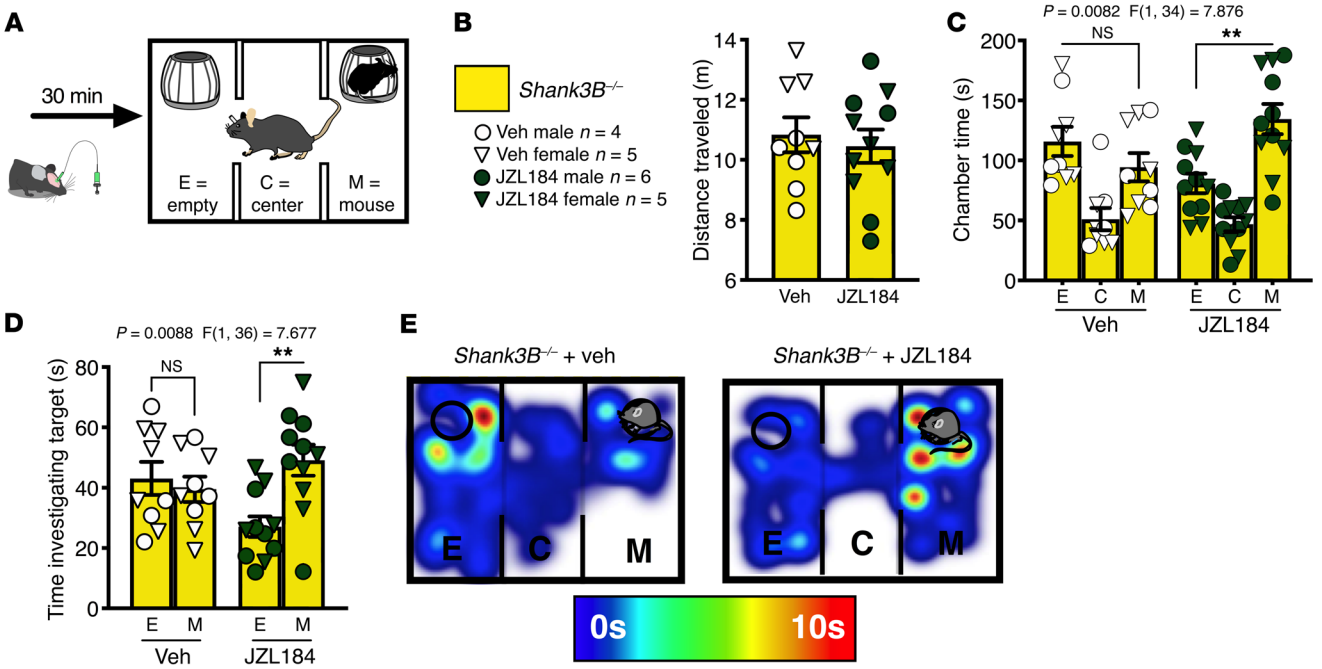

Figure 8. JZL184 microinfused into the NAc reverses the sociability deficit in *Shank3B*$^{-/-}$ animals. (**A**) Diagram of microinfusion experimental design. (**B**) JZL184 administered to the NAc did not alter distance traveled. (**C**) Veh-treated *Shank3B*$^{-/-}$ animals did not exhibit a preference for the mouse chamber (NS, $P = 0.8566$), while JZL184 increased social chamber preference (**$P = 0.0014$). (**D**) Additionally, Veh-treated *Shank3B*$^{-/-}$ did not have a preference for investigating the mouse cup while JZL184 increased investigation time (**$P = 0.0022$); Veh $n = 9$, JZL184 $n = 11$ (**B**–**D**). (**E**) Representative heatmaps of 3-chamber SI task. Data analyzed via unpaired, 2-tailed *t* test (**B**) or 2-way ANOVA with Holm-Šídák multiple-comparisons test (**C** and **D**). *P* and *F* values for chamber × drug interaction shown in **C** and **D**.

mice spent in the mouse chamber and time investigating the target mouse under the cup (Figure 8, C–E). Vehicle microinfusion did not result in increased time spent in the mouse-containing chamber or increase time in social investigation of the mouse relative to the empty cup. These data indicate local actions of JZL184 within the NAc are sufficient to normalize SI deficits in *Shank3B*$^{-/-}$ mice.

Given that elevating 2-AG selectively within the NAc was sufficient to increase social behavior in the *Shank3B*$^{-/-}$ mouse, we investigated the effects of JZL184 on synaptic signaling in the NAc as well as specifically after BLA-NAc optogenetic stimulation to gain insight into the potential mechanisms by which JZL184 may affect sociability in *Shank3B*$^{-/-}$ mice. First, we found no changes in the intrinsic excitability of NAc MSNs as measured by the number of action potentials generated per current injection, action potential threshold, resting potential, or input resistance between WT and *Shank3B*$^{-/-}$ mice (Supplemental Figure 6, A–D). However, we found that *Shank3B*$^{-/-}$ animals displayed a robust increase in sIPSC frequency (Figure 9A), but not amplitude (Figure 9B), as well as increased sEPSC frequency (Figure 9C), but not amplitude (Figure 9D), in the NAc. Moreover, we observed that JZL184 significantly reduced sIPSC and sEPSC frequency in the NAc of *Shank3B*$^{-/-}$ mice (Figure 9, A and C). In response to ex vivo BLA-NAc optogenetic stimulation, we observed no genotype-specific effects on either BLA-NAc oEPSCs or disynaptic feed-forward (FF) optically evoked inhibitory postsynaptic currents (oIPSCs) (Figure 9, E–H). However, JZL184 robustly decreased BLA-NAc FF oIPSC amplitude in *Shank3B*$^{-/-}$ but not WT mice (Figure 9, E and F). JZL184 did not affect BLA-NAc oEPSC amplitude in either *Shank3B*$^{-/-}$ or WT mice (Figure 9, G and H). These data suggest 2-AG augmentation could normalize social function in *Shank3B*$^{-/-}$ mice via modulation of BLA-NAc–elicited FF inhibition (possibly mediated via local GABAergic interneurons), which could ultimately result in disinhibition of NAc MSNs (Figure 10). This model could also explain increased sociability after BLA-NAc circuit inhibition in *Shank3B*$^{-/-}$ mice because reduced BLA glutamatergic drive to local NAc GABAergic interneurons would also disinhibit MSNs (Figure 10). How the balance of direct BLA excitation of NAc MSNs and local GABAergic interneurons is sculpted to ultimately direct optimal sociability remains to be determined.

Discussion

A main finding of the present study is that activation of the BLA-NAc glutamatergic circuit is sufficient to decrease sociability in the 3-chamber SI task, increase social avoidance in a naturalistic juvenile reciprocal interaction task, and reduce SI seeking in a social CPP assay. Previous studies have shown that glutamatergic projections from the BLA, including those to the ventral hippocampus (vHPC) and medial prefrontal cortex (mPFC), also decrease SI time when activated (53, 54). However, activation of BLA-vHPC and BLA-mPFC circuits also increases anxiety-like behavior (53, 55). Because social behavior deficits are often associated with increases in anxiety (44, 45), we measured the effects of BLA-NAc activation in anxiety-like behavior. However, we did not observe anxiogenic effects of BLA-NAc stimulation in the elevated plus maze or light-dark box assays. Interestingly however, we did observe increased immobility, a potential indicator of a fear

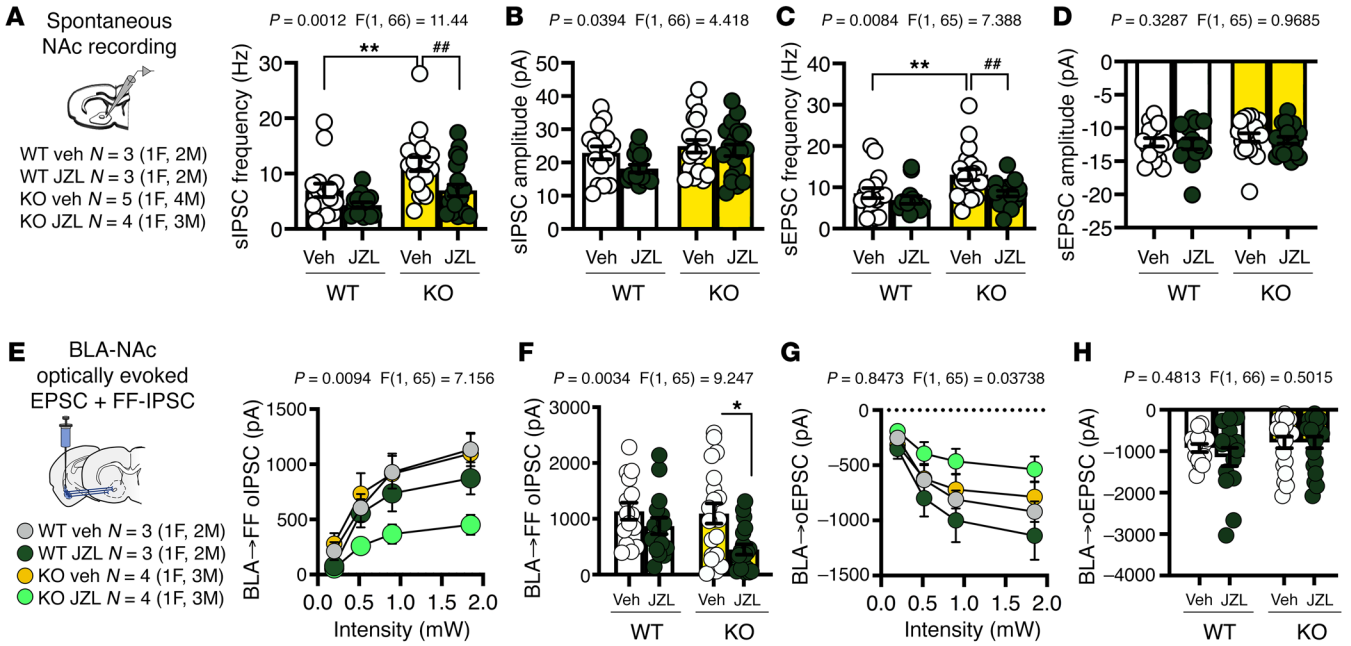

Figure 9. JZL184 significantly reduces sIPSC frequencies in the NAc and BLA-NAc feed-forward inhibition in *Shank3B*$^{-/-}$ mice. (**A**) sIPSC frequency on the NAc MSNs was significantly increased in *Shank3B*$^{-/-}$ compared with WT mice (**P = 0.0060) and was restored by JZL184 (##P = 0.0033). (**B**) There was no effect of *Shank3B*$^{-/-}$ on sIPSC amplitude. (**C**) sEPSC frequency was significantly increased in *Shank3B*$^{-/-}$ mice relative to WT animals (**P = 0.0084) and was restored by JZL184 (##P = 0.0060). (**D**) There was no effect of genotype or drug on sEPSC amplitude; WT + Veh n = 3, WT + JZL184 n = 3, KO + Veh n = 5, and KO + JZL184 n = 4 (**A**–**D**). (**E**) There was no difference between WT and *Shank3B*$^{-/-}$ BLA FF oIPSCs onto NAc cells. (**F**) However, at maximal stimulation (1.85 mW), JZL184 significantly reduced BLA FF oIPSCs onto NAc MSNs (*P = 0.0101). (**G** and **H**) There was no effect of JZL184 or genotype on BLA oEPSCs in the NAc across intensities; WT + Veh n = 3, WT + JZL184 n = 3, KO + Veh n = 4, and KO + JZL184 n = 4 (**E**–**H**). Data analyzed via 2-way ANOVA with Holm-Šídák multiple-comparisons test (**A**–**H**). P and F values for drug effect shown in **A**–**H**. M, males; F, females.

response, during BLA-NAc stimulation in the juvenile reciprocal SI task, suggesting reduced SI in this task may be secondary to fear or anxiety-like states. Alternatively, it is possible mice are remaining immobile to avoid SI because of the target mouse freely interacting with the test mouse, rather than being contained within a cup, as was the case in the 3-chamber SI task. Last, the BLA-NAc circuit has been strongly implicated in reward-seeking behavior, and stimulation of the BLA-NAc circuit is reinforcing (present data and refs. 24, 43). These data suggest BLA-NAc stimulation could reduce SI via an occlusion of the rewarding aspect of social behavior. However, BLA-NAc stimulation did not reduce interaction with a palatable nonsocial reward (Ensure) in our modified 3-chamber assay, arguing against this possibility. Taken together, these data suggest BLA-NAc glutamatergic circuit activation reduces sociability and social reward seeking, which are not likely secondary to increases in anxiety or mediated via occlusion of the rewarding effects of SI.

One possible explanation for how BLA-NAc activation results in social avoidance may relate to underlying BLA-NAc subcircuits. Specifically, previous studies have shown that activation of D2$^+$ MSNs directly in the NAc, and in vivo optogenetic activation of the cholecystokinin–expressing BLA neurons that project preferentially to NAc D2$^+$ MSNs, significantly decrease time in the SI zone after social defeat stress (24). In contrast, the reinforcing effects of BLA-NAc stimulation can be blocked by a D1 receptor antagonist (22), indicating BLA-NAc D1$^+$ MSN activation could underlie the rewarding effects of BLA-NAc circuit activation. Context-dependent differential engagement of these distinct subcircuits could explain parallel roles in reward and social avoidance observed after BLA-NAc circuit manipulations. Future studies directly examining and manipulating BLA-NAc subcircuit activity in social and nonsocial contexts may help clarify the neural mechanisms underlying BLA-NAc circuit effects on sociability and reward.

Given that BLA-NAc circuit activation reduces sociability, we next sought to explore molecular mechanisms that reduce BLA-NAc circuit activity in an attempt to reveal therapeutic approaches to increase social behavior. Previous work has demonstrated that activation of the CB1 receptor by eCBs, including 2-AG, dampens glutamatergic activity (46) and has a functional role in social behavior via modulation of both NAc signaling and endogenous BLA-NAc activity (9, 10, 12, 24, 56). Therefore, we investigated whether 2-AG signaling modulated BLA-NAc glutamatergic transmission. Indeed, we show that CB1 receptor activation reduced glutamate release at BLA-NAc synapses and that enhancement of 2-AG signaling via MAGL inhibition by JZL184 reduced aEPSC frequency at BLA-NAc D1$^+$ and putative D2$^+$ MSNs. It is noteworthy that these results are in contrast to a recent study indicating cannabinoid signaling selectively modulates BLA-NAc D2$^+$ MSN synapses (24). Consistent with the ability of CB1 activation and 2-AG augmentation to reduce optogenetically elicited glutamatergic signaling efficacy at BLA-NAc synapses ex vivo, we showed that systemic JZL184 administration prevented the decreased sociability elicited by BLA-NAc optogenetic stimulation in vivo. Our

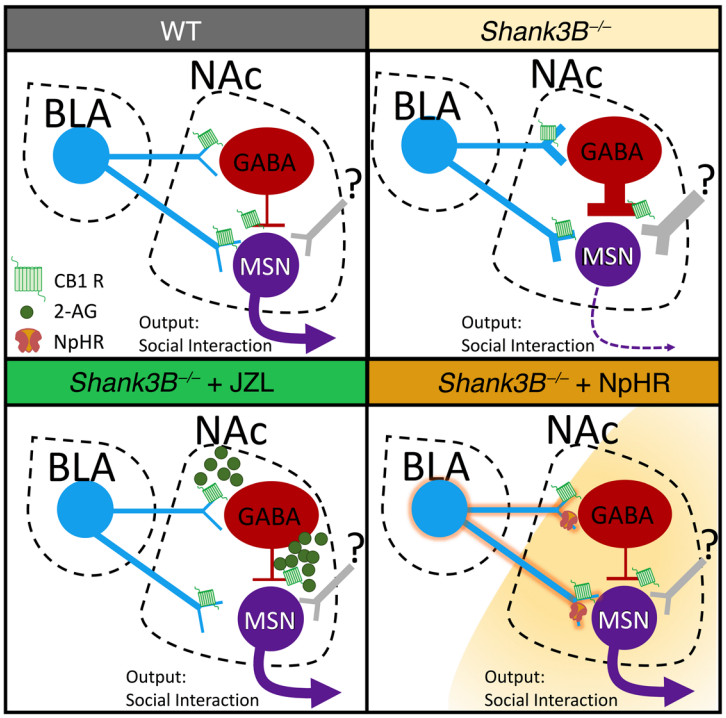

Figure 10. Working model of eCB/BLA/NAc interactions in *Shank3B*$^{-/-}$ mice. *Shank3B*$^{-/-}$ mice exhibit increased sEPSC and sIPSC frequency onto MSNs in the NAc relative to WT mice and exhibit social impairment. In *Shank3B*$^{-/-}$ mice treated with systemic or intra-NAc JZL184 to increase 2-AG levels, sEPSC and sIPSC frequency is normalized as is BLA-NAc FF inhibition, resulting in a reduction in social deficits. *Shank3B*$^{-/-}$ mice with optogenetic inhibition of BLA-NAc circuit function are hypothesized to have similarly reduced FF inhibition and reduced overall glutamatergic drive to GABA interneurons and MSNs, which also reduces social deficits.

data suggest pharmacological 2-AG augmentation could serve as a therapeutic approach to increase sociability under pathological conditions associated with amygdala-NAc circuit hyperactivity.

Although we show that activation of the BLA-NAc circuit is sufficient to reduce SI behavior, we also show that activity is not necessary for the physiological expression of social behavior because optogenetic inhibition of the circuit did not alter sociability under basal conditions. This finding differentiates the BLA-NAc circuit from other BLA circuits, such as BLA-vHPC, which bidirectionally alter social behavior (54). Although our data suggest BLA-NAc activity is not physiologically recruited to regulate sociability, it is possible that BLA-NAc circuit inhibition could increase or normalize sociability in mice with preexisting social impairment. Indeed, we found that inhibition of the BLA-NAc circuit robustly increased social behavior in the *Shank3B*$^{-/-}$ mouse, a model of ASD that has a well-established social deficit (39, 51, 52). Consistent with our data, clinical reports have demonstrated that the amygdala is hyperfunctional in patients with ASDs during anticipation of social cues and that the NAc of patients with ASDs has increased functional connectivity relative to typically developing peers (17, 18, 57). Continued research into the functional connectivity of the BLA-NAc circuit in patients with ASD and additional preclinical mouse models of ASD are needed to fully understand the role of the BLA-NAc circuit in ASD-associated social deficits.

We also showed that 2-AG augmentation via systemic JZL184 administration reversed both social and restricted, repetitive behavior deficits in *Shank3B*$^{-/-}$ mice. Additionally, direct administration of JZL184 into the NAc was sufficient to rescue social behavioral deficits in *Shank3B*$^{-/-}$ mice. Taken together, these data add to the growing body of evidence suggesting pharmacological eCB augmentation could serve as a therapeutic approach for treating ASD and ASD-associated syndromes (47, 58–62). Currently there are no FDA-approved pharmacological treatments for ASD, and current medications to improve social deficits are limited. Given the recent advancement of MAGL inhibitors to early clinical trials (63, 64), our data could support examination of MAGL inhibitors for the treatment of social deficits in ASD and other disorders characterized by social domain deficits.

In the present study we show that, relative to WT littermates, *Shank3B*$^{-/-}$ animals have increased sIPSC and sEPSC frequency, but not amplitude, in the NAc, revealing increased GABA and glutamate release probability but no changes in the intrinsic excitability of NAc MSNs. Interestingly, JZL184 restored both sIPSC and sEPSC frequency to that of WT levels. These data provide a potential mechanism for the restoration of social function elicited via systemic and intra-NAc JZL184 infusions in *Shank3B*$^{-/-}$. Our findings of increased sIPSC frequency in the NAc of the *Shank3B*$^{-/-}$ animals are consistent with previous findings showing hypoactivity of the NAc during SI in a complete *Shank3*-knockout model (41). Taken together, these data may reveal a convergent mechanism of heightened GABAergic activity in the NAc of *Shank3*$^{-/-}$ models. Future studies of NAc activity in additional ASD models may provide insight into the role of NAc synaptic physiology in social behavior more broadly.

Because we found SI deficits were normalized by BLA-NAc circuit inhibition in *Shank3B*$^{-/-}$ mice, we also analyzed BLA-NAc circuit physiology in *Shank3B*$^{-/-}$ animals. Unexpectedly, we found no measurable differences in BLA input into the NAc in *Shank3B*$^{-/-}$ mice compared to WT animals as oEPSC and FF oIPSC amplitudes were not different between genotypes; however, JZL184 was able to reduce FF oIPSC amplitude in *Shank3B*$^{-/-}$, but not WT, mice. These data seemingly contrast with our finding showing inhibition of the BLA-NAc restored sociability behavior in *Shank3B*$^{-/-}$ animals because glutamatergic drive onto NAc

neurons was not altered. However, it is possible that inhibition of GABAergic interneurons in the NAc of *Shank3B*$^{-/-}$ animals, by either NpHR-induced reductions in FF inhibition or JZL184 application, was sufficient to restore social function. One possible way that JZL184 could improve SI is via inhibition of glutamatergic BLA synapses and GABAergic fast-spiking interneurons (FSIs) onto MSNs, both of which are regulated by CB1 receptors at the presynaptic level (Figure 10) (26, 65, 66). Increases in 2-AG may therefore inhibit activation of NAc FSIs in response to BLA stimulation as well as inhibit GABAergic release from FSIs. Because FSIs in the NAc have been shown to gate impulsive behavior in mice (67), we hypothesize that JZL184 inhibition of FSIs' signaling could promote SI via increasing directed social behavior output similarly. Additionally, reductions in FSI inhibition of NAc MSNs could allow for restoration of proper signaling from other NAc inputs, such as the prefrontal cortex, which could be dysregulated in *Shank3B*$^{-/-}$ mice. Further investigation into the role of FSIs, GABAergic circuitry, and additional glutamatergic inputs to the NAc in the *Shank3B*$^{-/-}$ model, as they relate to social behavior, may uncover additional synaptic mechanisms contributing to social deficits in ASDs.

In summary, we show that BLA-NAc circuit activation reduces sociability and is highly regulated by 2-AG–mediated eCB signaling. We further show that systemic and NAc-specific 2-AG augmentation and optogenetic BLA-NAc circuit inhibition normalize social deficits in the *Shank3B*$^{-/-}$ model of ASDs. We hypothesize that 2-AG augmentation reduces social deficits in *Shank3B*$^{-/-}$ mice via normalization of hyperactive GABAergic and glutamatergic signaling in the NAc and via reductions in BLA-elicited FF inhibition onto NAc MSNs. These data reveal the BLA-NAc circuit as a critical regulator of social function and suggest pharmacological 2-AG augmentation could represent a promising approach to the treatment of social domain symptoms in ASDs.

Methods

Animals

Mice were housed on a 12-hour light/12-hour dark cycle with lights on at 0600 hours. All experiments were conducted during the light phase. Food and water were available ad libitum. Mice on a C57BL/6J background were used for all experiments. WT (*a Tyrp1*^{b} *Pmel*^{si}/J) mice were ordered from The Jackson Laboratory (JAX; stock 00064) at 5 weeks of age. Male and female *Shank3B*$^{+/-}$ (B6.129-*Shank3*^{tm2Gfng}/J) mice were ordered from JAX (stock 017688) and bred in-house. Male and female transgenic bacterial artificial chromosome (BAC) *Drd1a-tdTomato* (stock 016204) and BAC Drd2-EGFP (stock 0302554) mice were obtained from JAX and bred to C57BL/6J WT females.

Viruses

For in vivo optogenetic studies we used AAV5-CaMKIIa-hChR2(H134)-EYFP for optical excitation or AAV5-CaMKIIa-eNpHR3.0-EYFP for optical inhibition and AAV5-CaMKIIa-EYFP (250 nL, University of North Carolina at Chapel Hill Vector Core) as a control in all studies.

Stereotaxic surgery

Male and female mice at 5–8 weeks old underwent unilateral or bilateral stereotaxic surgery, as indicated in the figures, under isoflurane anesthesia. Viruses were infused into the BLA (anterior/posterior [AP]: –1.25, medial/lateral [ML]: ±3.25, dorsal/ventral [DV]: 5.05) at a rate of 100 nL/min. At least 4 weeks following viral injection, mice underwent unilateral or bilateral fiber optic implantation. Implants were lowered to the ipsilateral NAc of the viral surgery (AP: 1.25, ML: ±0.55, DV: 4.10, +10° or –10° tilt for bilateral implants) (0.20 mm/s). For microinfusion studies, bilateral, stainless-steel infusion guide cannulas (26 gauge, cut to 3-mm length, 2 mm center-to-center distance, C235GS-5-2.0/SPC- Plastics One) were placed above the NAc (AP: 1.35, ML: ±1.00, DV: 3.00) and fitted with a dummy cannula (C235DCS-5/SPC, Plastics One) and dust cap (303DC/1 Plastics One). Implants were secured with dental cement. Animals recovered for at least 1 week before any experimental manipulation.

Electrophysiology

Acute slice preparation and whole-cell patch-clamp recordings were performed similarly to those previously described (68–70). MSNs in the NAc were identified based on resting membrane potential and visual appearance (size, morphology) at original magnification ×40 with an immersion objective with differential interference contrast microscopy. Putative D1 receptor or D2 receptor neurons were identified by the presence or absence of fluorophore expression in BAC-transgenic mice expressing tdTomato under the D1 receptor promoter or GFP under the D2 receptor promoter. For more detailed electrophysiological methods, see Supplemental Methods.

Behavior testing

All mice were single housed with the exception of animals tested in the repetitive grooming assay. All experiments were conducted at least 48 hours apart. *Shank3B*$^{-/-}$ animals were run in parallel with WT littermate controls. All animals were handled at least 3 days before testing.

Three-chamber SI test. After a 10-minute habituation phase, the test mouse was permitted to freely explore the arena containing a sex-matched, juvenile (4- to 6-week-old) mouse inside 1 inverted pencil cup and an empty inverted pencil cup in the opposite chamber for the test phase (5 minutes). When *Shank3B*$^{-/-}$ animals were used, animals were paired with age-matched, sex-matched targets and given a 5-minute habituation while restricted to the center chamber, as previously described (39). For in vivo optogenetic studies, stimulation was delivered during the test phase unless otherwise noted (Supplemental Figure 2, A and B). Videos were coded post hoc for time investigating each cup by 2 blinded coders. Time investigating represents time in which the test mouse is sniffing or interacting with the cup.

Ensure 3-chamber task. Animals were trained for 3 consecutive days in their home cage to drink commercially available Ensure. On test day, animals were placed in the 3-chamber apparatus (as described above). An Ensure-filled sipper bottle was affixed to an inverted pencil cup so that the animals could easily reach and drink from the sipper. Stimulation was turned on and animals were permitted to freely explore the apparatus for 5 minutes. Videos were analyzed post hoc for time drinking Ensure or time investigating (sniffing or interacting with) the empty cup by 2 blinded coders.

Grooming behavior assay. Animals were placed into an empty, clean, novel cage for 15 minutes. Videos were recorded during the interaction and analyzed post hoc by 2 independent, blinded coders beginning after a 5-minute habituation period.

Juvenile reciprocal SI test. Animals were permitted to freely interact with a sex-matched, juvenile mouse (~4 weeks old) for 10 minutes in a clean, novel cage. Videos were analyzed post hoc by 2 independent, blinded coders.

RtPP. When animals entered a randomly assigned chamber, light stimulation was delivered; stimulation ended when animals left the stimulation chamber. Animals were tested for 5 minutes.

Social CPP. We used a 3-chamber apparatus with 2 distinct chambers (dots and stripes) and a connecting corridor. After a pretest trial (10 minutes), mice were assigned in a counterbalanced, unbiased manner into either the dotted or striped chamber with a novel, juvenile, sex-matched mouse for 10 minutes, immediately followed by 10 minutes in the opposite chamber alone. This repeated for 3 consecutive days total. Finally, on test day, light stimulation was turned on, and animals were able to freely move in the apparatus for 10 minutes.

For complete behavioral methods, see Supplemental Methods.

In vivo optogenetic stimulation

Stimulation patterns were delivered from the PlexBright 4 Channel Optogenetic Controller and controlled by Radiant v2 software (Plexon). The optogenetics controller box was attached to the PlexBright Dual LED rotatable commutator, in which a blue (465 nm) or orange (620 nm) LED light was affixed (Plexon). PlexBright Optical Patch Cables (0.5 NA) were then attached to the commutator (Plexon). In blue light stimulation studies, animals received 20-Hz blue light stimulation (Plexon) in a 5 seconds on, 5 seconds off, pattern at 10–13 mW. For inhibition studies, animals received a constant orange light (~10 mW). One week following implantation surgery, mice were habituated to false patch cables in 20-minute bins for 3 consecutive days. On test day, the patch cable was connected to the fiber optic implants, and animals were habituated for at least 5 minutes before the start of any behavior test.

Microinfusion studies

After 7 days of recovery from stereotaxic surgery, animals were habituated to handling for 3 consecutive days in which animals were restrained in increasing amounts (30 seconds, 60 seconds, 120 seconds) and dummy cannula were replaced daily to prevent blocking and habituate animals to restraint. JZL184 was bilaterally infused into the NAc using a bilateral, 4-mm cut length internal infusion cannula (C235IS-5/SPC, Plastics One) at a dose of 0 or 5 μg/L and at a volume of 0.2 μL per hemisphere over 1 minute as previously described (71). Animals were placed into the 3-chamber SI task 30 minutes after infusion.

Histology and imaging

After animals completed behavior experiments, brain tissue was collected to validate implant and viral placement. For validation experiments, brain tissue slices were mounted in VECTASHIELD with DAPI (Vector Laboratories, Maravai LifeSciences) onto charged slides and sealed with a clear nail polish. Images were collected using an upright ZEISS Axio Imager M2 epifluorescent microscope at 5× and 20× objectives.

Exclusion criteria

For all viral and implant studies, animals were excluded based on a priori standards. The injection site of all viral injections was identified by the presence of GFP or enhanced YFP fluorescent marker. For all fiber optic implantations, location was determined by implantation track. Animals were excluded from all data sets if the viral expression or implantation was not in the targeted regions. For all in vivo studies the location of the viral expression and implantation is displayed in Supplemental Figure 1. *Shank3B*$^{-/-}$ and WT controls were genotyped following sacrifice for confirmation. Cells were excluded from all analyses for 4 reasons: (a) if the holding current dropped below –200 pA at any time during the recording, (b) if the access resistance was more than 20 MΩ, (c) if the access resistance fluctuated by more than 20% throughout the recording, or (d) if there was no optogenetically evoked response. In all data sets, data were analyzed using Grubbs' outlier test ($\alpha = 0.05$) and removed accordingly. If animals were excluded from a behavioral test for outlying data points, all data collected from the animal in the experiment were removed.

Statistics

Data are represented as mean ± SEM, with individual plot points overlaid on a mean bar graph. Statistical analysis was conducted using Prism 8 (GraphPad). Statistical tests and parameters are indicated in figure legends. Significance was set at $\alpha = 0.05$. A P value less than 0.05 was considered significant; t tests were 2 tailed.

Study approval

All studies were carried out in accordance with the National Institutes of Health (NIH) *Guide for the Care and Use of Laboratory Animals* (National Academies Press, 2011) and approved by the Vanderbilt University Institutional Animal Care and Use Committee.

For full methods, please see Supplemental Methods.

Author contributions

SP and OMF conceived the study, designed experiments, and cowrote the paper. OMF performed experiments and acquired and analyzed data in the laboratory of SP. RB, DJM, and NDH completed, assisted in the design of, and analyzed ex vivo electrophysiological experiments and data in the laboratory of SP, while BDT completed, designed, and analyzed electrophysiological experiments and data in the lab of BAG. CAG and OMF designed and completed microinfusion experiments in the laboratory of BAG. VK, JJB, and MA assisted in the completion of experiments. VK, JKA, and MPM coded behavioral data.

Acknowledgments

This work was supported by the Simons Foundation and NIH grant MH107435. The authors would like to thank Rafael Perez for assistance with figure and graphical abstract design. The authors would also like to thank Vanderbilt University's Mouse Behavior Core and John Allison for assistance with behavior paradigms and equipment. The content is solely the responsibility of the authors and does not necessarily represent the official views of the NIH.

Address correspondence to: Sachin Patel, Department of Psychiatry and Behavioral Sciences, Vanderbilt University Medical Center, Medical Research Building IV, Room 8425B, 2213 Garland Avenue, Nashville, Tennessee 37232, USA. Phone: 615.936.7768; Email: sachin.patel@vanderbilt.edu.

1. American Psychiatric Association. *Diagnostic and statistical manual of mental disorders*. 5th ed. Washington, DC: American Psychiatric Association; 2013.
2. Aman M, et al. Tolerability, safety, and benefits of risperidone in children and adolescents with autism: 21-month follow-up after 8-week placebo-controlled trial. *J Child Adolesc Psychopharmacol*. 2015;25(6):482–493.
3. McDougle CJ, Epperson CN, Pelton GH, Wasylink S, Price LH. A double-blind, placebo-controlled study of risperidone addition in serotonin reuptake inhibitor-refractory obsessive-compulsive disorder. *Arch Gen Psychiatry*. 2000;57(8):794–801.
4. Broadstock M, Doughty C, Eggleston M. Systematic review of the effectiveness of pharmacological treatments for adolescents and adults with autism spectrum disorder. *Autism*. 2007;11(4):335–348.
5. Fukuda T, Sugie H, Ito M, Sugie Y. [Clinical evaluation of treatment with fluvoxamine, a selective serotonin reuptake inhibitor in children with autistic disorder]. *No To Hattatsu*. 2001;33(4):314–318.
6. Yokoyama H, Hirose M, Haginoya K, Munakata M, Iinuma K. [Treatment with fluvoxamine against self-injury and aggressive behavior in autistic children]. *No To Hattatsu*. 2002;34(3):249–253.
7. Shyn SI, et al. Novel loci for major depression identified by genome-wide association study of Sequenced Treatment Alternatives to Relieve Depression and meta-analysis of three studies. *Mol Psychiatry*. 2011;16(2):202–215.
8. Hoch E, et al. How effective and safe is medical cannabis as a treatment of mental disorders? A systematic review. *Eur Arch Psychiatry Clin Neurosci*. 2019;269(1):87–105.
9. Wei D, Lee D, Li D, Daglian J, Jung KM, Piomelli D. A role for the endocannabinoid 2-arachidonoyl-sn-glycerol for social and high-fat food reward in male mice. *Psychopharmacology (Berl)*. 2016;233(10):1911–1919.
10. Manduca A, et al. Interacting cannabinoid and opioid receptors in the nucleus accumbens core control adolescent social play. *Front Behav Neurosci*. 2016;10:211.
11. Trezza V, et al. Endocannabinoids in amygdala and nucleus accumbens mediate social play reward in adolescent rats. *J Neurosci*. 2012;32(43):14899–14908.
12. Wei D, et al. Endocannabinoid signaling mediates oxytocin-driven social reward. *Proc Natl Acad Sci U S A*. 2015;112(45):14084–14089.
13. Aragona BJ, et al. Nucleus accumbens dopamine differentially mediates the formation and maintenance of monogamous pair bonds. *Nat Neurosci*. 2006;9(1):133–139.
14. Francis TC, et al. Nucleus accumbens medium spiny neuron subtypes mediate depression-related outcomes to social defeat stress. *Biol Psychiatry*. 2015;77(3):212–222.
15. van der Kooij MA, et al. Diazepam actions in the VTA enhance social dominance and mitochondrial function in the nucleus accumbens by activation of dopamine D1 receptors. *Mol Psychiatry*. 2018;23(3):569–578.
16. Gunaydin LA, et al. Natural neural projection dynamics underlying social behavior. *Cell*. 2014;157(7):1535–1551.
17. Di Martino A, et al. Aberrant striatal functional connectivity in children with autism. *Biol Psychiatry*. 2011;69(9):847–856.
18. Dichter GS, Felder JN, Green SR, Rittenberg AM, Sasson NJ, Bodfish JW. Reward circuitry function in autism spectrum disorders. *Soc Cogn Affect Neurosci*. 2012;7(2):160–172.
19. Varghese M, et al. Autism spectrum disorder: neuropathology and animal models. *Acta Neuropathol*. 2017;134(4):537–566.
20. Millan EZ, Kim HA, Janak PH. Optogenetic activation of amygdala projections to nucleus accumbens can arrest conditioned and unconditioned alcohol consummatory behavior. *Neuroscience*. 2017;360:106–117.
21. Namburi P, et al. A circuit mechanism for differentiating positive and negative associations. *Nature*. 2015;520(7549):675–678.
22. Stuber GD, et al. Excitatory transmission from the amygdala to nucleus accumbens facilitates reward seeking. *Nature*. 2011;475(7356):377–380.
23. Ambroggi F, Ishikawa A, Fields HL, Nicola SM. Basolateral amygdala neurons facilitate reward-seeking behavior by exciting nucleus accumbens neurons. *Neuron*. 2008;59(4):648–661.
24. Shen CJ, et al. Cannabinoid CB_1 receptors in the amygdalar cholecystokinin glutamatergic afferents to nucleus accumbens modulate depressive-like behavior. *Nat Med*. 2019;25(2):337–349.
25. Beyeler A, et al. Organization of valence-encoding and projection-defined neurons in the basolateral amygdala. *Cell Rep*. 2018;22(4):905–918.
26. Yu J, et al. Nucleus accumbens feedforward inhibition circuit promotes cocaine self-administration. *Proc Natl Acad Sci U S A*. 2017;114(41):E8750–E8759.
27. Bercovici DA, Princz-Lebel O, Tse MT, Moorman DE, Floresco SB. Optogenetic dissection of temporal dynamics of amygdala-striatal interplay during risk/reward decision making. *eNeuro*. 2018;5(6):ENEURO.0422-18.2018.
28. Kazdoba TM, Leach PT, Yang M, Silverman JL, Solomon M, Crawley JN. Translational mouse models of autism: advancing toward pharmacological therapeutics. *Curr Top Behav Neurosci*. 2016;28:1–52.
29. Kolevzon A, et al. Phelan-McDermid syndrome: a review of the literature and practice parameters for medical assessment and monitoring. *J Neurodev Disord*. 2014;6(1):39.
30. Phelan K, McDermid HE. The 22q13.3 deletion syndrome (Phelan-McDermid syndrome). *Mol Syndromol*. 2012;2(3–5):186–201.
31. Vorstman JA, Staal WG, van Daalen E, van Engeland H, Hochstenbach PF, Franke L. Identification of novel autism candidate regions through analysis of reported cytogenetic abnormalities associated with autism. *Mol Psychiatry*. 2006;11(1):18–28.
32. Vorstman JAS, et al. The 22q11.2 deletion in children: high rate of autistic disorders and early onset of psychotic symptoms. *J Am Acad Child Adolesc Psychiatry*. 2006;45(9):1104–1113.
33. Monteiro P, Feng G. SHANK proteins: roles at the synapse and in autism spectrum disorder. *Nat Rev Neurosci*. 2017;18(3):147–157.
34. Naisbitt S, et al. Shank, a novel family of postsynaptic density proteins that binds to the NMDA receptor/PSD-95/GKAP complex and cortactin. *Neuron*. 1999;23(3):569–582.
35. Boccuto L, et al. Prevalence of SHANK3 variants in patients with different subtypes of autism spectrum disorders. *Eur J Hum Genet*. 2013;21(3):310–316.
36. Durand CM, et al. Mutations in the gene encoding the synaptic scaffolding protein SHANK3 are associated with autism spectrum disorders. *Nat Genet*. 2007;39(1):25–27.
37. Leblond CS, et al. Meta-analysis of SHANK mutations in autism spectrum disorders: a gradient of severity in cognitive impairments. *PLoS Genet*. 2014;10(9):e1004580.
38. Moessner R, et al. Contribution of SHANK3 mutations to autism spectrum disorder. *Am J Hum Genet*. 2007;81(6):1289–1297.
39. Peça J, et al. Shank3 mutant mice display autistic-like behaviours and striatal dysfunction. *Nature*. 2011;472(7344):437–442.
40. Zhou Y, et al. Atypical behaviour and connectivity in SHANK3-mutant macaques. *Nature*. 2019;570(7761):326–331.
41. Wang X, et al. Altered mGluR5-Homer scaffolds and corticostriatal connectivity in a Shank3 complete knockout model of autism. *Nat Commun*. 2016;7:11459.
42. Stamatakis AM, et al. Simultaneous optogenetics and cellular resolution calcium imaging during active behavior using a miniaturized microscope. *Front Neurosci*. 2018;12:496.
43. Stuber GD, et al. Excitatory transmission from the amygdala to nucleus accumbens facilitates reward seeking. *Nature*. 2011;475(7356):377–380.
44. Sukhodolsky DG, et al. Parent-rated anxiety symptoms in children with pervasive developmental disorders: frequency and association with core autism symptoms and cognitive functioning. *J Abnorm Child Psychol*. 2008;36(1):117–128.
45. Allsop SA, Vander Weele CM, Wichmann R, Tye KM. Optogenetic insights on the relationship between anxiety-related behaviors and social deficits. *Front Behav Neurosci*. 2014;8:241.
46. Araque A, Castillo PE, Manzoni OJ, Tonini R. Synaptic functions of endocannabinoid signaling in health and disease. *Neuropharmacology*. 2017;124:13–24.
47. Wei D, et al. Enhancement of anandamide-mediated endocannabinoid signaling corrects autism-related social impairment. *Cannabis Cannabinoid Res*. 2016;1(1):81–89.
48. Trusel M, et al. Coordinated regulation of synaptic plasticity at striatopallidal and striatonigral neurons orchestrates motor control. *Cell Rep*. 2015;13(7):1353–1365.
49. Grueter BA, Brasnjo G, Malenka RC. Postsynaptic TRPV1 triggers cell type-specific long-term depression in the nucleus accumbens. *Nat Neurosci*. 2010;13(12):1519–1525.
50. Kreitzer AC, Malenka RC. Striatal plasticity and basal ganglia circuit function. *Neuron*. 2008;60(4):543–554.
51. Guo B, et al. Anterior cingulate cortex dysfunction underlies social deficits in Shank3 mutant mice. *Nat Neurosci*. 2019;22(8):1223–1234.

52. Mei Y, et al. Adult restoration of Shank3 expression rescues selective autistic-like phenotypes. *Nature*. 2016;530(7591):481–484.
53. Felix-Ortiz AC, Burgos-Robles A, Bhagat ND, Leppla CA, Tye KM. Bidirectional modulation of anxiety-related and social behaviors by amygdala projections to the medial prefrontal cortex. *Neuroscience*. 2016;321:197–209.
54. Felix-Ortiz AC, Tye KM. Amygdala inputs to the ventral hippocampus bidirectionally modulate social behavior. *J Neurosci*. 2014;34(2):586–595.
55. Felix-Ortiz AC, Beyeler A, Seo C, Leppla CA, Wildes CP, Tye KM. BLA to vHPC inputs modulate anxiety-related behaviors. *Neuron*. 2013;79(4):658–664.
56. Manduca A, Servadio M, Damsteegt R, Campolongo P, Vanderschuren LJ, Trezza V. Dopaminergic neurotransmission in the nucleus accumbens modulates social play behavior in rats. *Neuropsychopharmacology*. 2016;41(9):2215–2223.
57. Dichter GS, Richey JA, Rittenberg AM, Sabatino A, Bodfish JW. Reward circuitry function in autism during face anticipation and outcomes. *J Autism Dev Disord*. 2012;42(2):147–160.
58. Jacome-Sosa M, et al. Vaccenic acid suppresses intestinal inflammation by increasing anandamide and related N-acylethanolamines in the JCR:LA-cp rat. *J Lipid Res*. 2016;57(4):638–649.
59. Qin M, Zeidler Z, Moulton K, Krych L, Xia Z, Smith CB. Endocannabinoid-mediated improvement on a test of aversive memory in a mouse model of fragile X syndrome. *Behav Brain Res*. 2015;291:164–171.
60. Kerr DM, Gilmartin A, Roche M. Pharmacological inhibition of fatty acid amide hydrolase attenuates social behavioural deficits in male rats prenatally exposed to valproic acid. *Pharmacol Res*. 2016;113(pt A):228–235.
61. Servadio M, et al. Targeting anandamide metabolism rescues core and associated autistic-like symptoms in rats prenatally exposed to valproic acid. *Transl Psychiatry*. 2016;6(9):e902.
62. Doenni VM, Gray JM, Song CM, Patel S, Hill MN, Pittman QJ. Deficient adolescent social behavior following early-life inflammation is ameliorated by augmentation of anandamide signaling. *Brain Behav Immun*. 2016;58:237–247.
63. Granchi C, Caligiuri I, Minutolo F, Rizzolio F, Tuccinardi T. A patent review of Monoacylglycerol Lipase (MAGL) inhibitors (2013-2017). *Expert Opin Ther Pat*. 2017;27(12):1341–1351.
64. Clapper JR, et al. Monoacylglycerol lipase inhibition in human and rodent systems supports clinical evaluation of endocannabinoid modulators. *J Pharmacol Exp Ther*. 2018;367(3):494–508.
65. Yu J, et al. Nucleus accumbens feedforward inhibition circuit promotes cocaine self-administration. *Proc Natl Acad Sci U S A*. 2017;114(41):E8750–E8759.
66. Manz KM, Baxley AG, Zurawski Z, Hamm HE, Grueter BA. Heterosynaptic GABAB receptor function within feedforward microcircuits gates glutamatergic transmission in the nucleus accumbens core. *J Neurosci*. 2019;39(47):9277–9293.
67. Pisansky MT, Lefevre EM, Retzlaff CL, Trieu BH, Leipold DW, Rothwell PE. Nucleus accumbens fast-spiking interneurons constrain impulsive action. *Biol Psychiatry*. 2019;86(11):836–847.
68. Hartley ND, et al. Dynamic remodeling of a basolateral-to-central amygdala glutamatergic circuit across fear states. *Nat Neurosci*. 2019;22(12):2000–2012.
69. Bluett RJ, et al. Endocannabinoid signalling modulates susceptibility to traumatic stress exposure. *Nat Commun*. 2017;8:14782.
70. Turner BD, Rook JM, Lindsley CW, Conn PJ, Grueter BA. $mGlu_1$ and $mGlu_5$ modulate distinct excitatory inputs to the nucleus accumbens shell. *Neuropsychopharmacology*. 2018;43(10):2075–2082.
71. Hartley ND, Gunduz-Cinar O, Halladay L, Bukalo O, Holmes A, Patel S. 2-arachidonoylglycerol signaling impairs short-term fear extinction. *Transl Psychiatry*. 2016;6:e749.